ELSEVIER

Applied Mathematical Modelling 25 (2001) 1071–1087

APPLIED MATHEMATICAL MODELLING

www.elsevier.com/locate/apm

A transfer function model to describe odor causing VOCs transport in a ventilated airspace with mixing/adsorption heterogeneity

Chung-Min Liao [a,*], Jein-Wen Chen [a], Jui-Sheng Chen [b], Huang-Min Liang [a]

[a] *Department of Agricultural Engineering, National Taiwan University, Taipei, Taiwan 10617, ROC*
[b] *Department of Environmental Engineering and Sanitation, Foo-Yin Institute of Technology, Kaohsiung, Taiwan 831, ROC*

Received 12 May 2000; received in revised form 30 November 2000; accepted 12 February 2001

Abstract

The ability of a transfer function modeling technique is evaluated to explain the odor causing VOCs (VOC-odor) transport processes influenced by heterogeneity of adsorption surface of ambient aerosol and air mixing pattern in a ventilated airspace. An advection–reaction impulse/step response function is used to generalize the dynamic transport of VOC-odor in heterogeneous mixing/adsorption ventilated airspace. The system process presented by an ensemble transfer function is solved analytically in the Laplace domain. The model requires the specification of probability density function (pdf) for residence time of airflow and for both equilibrium linear partitioning and first-order mass transfer rate parameters of gas/solid phase to quantify the specific air mixing pattern and transport processes. The model predicts the ensemble mean VOC-odor concentrations for a variety of adsorption kinetics and mixing pattern combinations as a function of the boundary impulse/step response inputs as well as residence time and adsorption rate statistics. The general behavior of output VOC-odor profiles is analyzed through the effects of mean adsorption rate coefficient, mean linear partitioning constant, mixing efficiency, mean residence time and coefficient of variations of both linear partitioning and rate coefficients. This study indicates that when mixing/adsorption heterogeneity exists, simple complete mixing assumption and simple distribution of rate constant are inherently not sufficient to represent a more generally distributed mixing/adsorption process of VOC-odor transport in a ventilated airspace.

Keywords: Transfer function; Mixing; Adsorption; Heterogeneity; Odor; VOCs

1. Introduction

The transport of odor causing volatile organic compounds (VOC-odor) generated from stored manure pit in a ventilated animal housing is increasingly the focus of research in bioenvironmental control engineering [1–6]. The transport processes of VOC-odor in a highly dusty livestock building environment are usually subjected to the rate limitation of mass transfer and the complex interactions among VOC-odor, ambient airborne dust, and dust-borne VOC-odor in a heterogeneous air mixing airspace.

* Corresponding author. Fax: +886-223626433.
E-mail address: cmliao@ccms.ntu.edu.tw (C.-M. Liao).

0307-904X/01/$ - see front matter
PII: S0307-904X(01)00032-4

Notation

a, b	positive constants in the linear free-energy relationships
$c(x,t)$	VOC-odor concentration (kg m^{-3})
C_0	initial concentration of VOC-odor (kg m^{-3})
$C^*(T,X)$	dimensionless variable of VOC-odor concentration
$\hat{C}^*(X,s)$	Laplace-transformed $C^*(T, X)$
$\hat{C}(X,s)$	ensemble mean of $\hat{C}^*(X,s)$
$\mathrm{CV}_k, \mathrm{CV}_\tau$	coefficients of variations of K and τ
$E[\cdot]$	mathematical expectation operator
$h(t)$	density function
$\hat{h}(s)$	transfer function for the rate-limiting processes
$\hat{H}(s)$	ensemble mean of $\hat{h}(s)$
k	adsorption rate coefficient (h^{-1})
k_d	linear partition coefficient between gas and solid phases at sorption equilibrium (m^3 kg^{-1})
K	dimensionless adsorption rate coefficient
$\bar{K}$	mean of gamma distribution of K
K_D	dimensionless equilibrium linear partitioning coefficient
$\bar{K}_\mathrm{D}$	mean linear partitioning coefficient
L_0	distance from face of outlet (m)
P_d	gamma pdf of K_D
P_{dk}	bivariate pdf of K_D and K
P_k	gamma pdf of K
P_τ	gamma pdf of τ
Q	volumetric airflow rate (m^3 s^{-1})
$q(x,t)$	concentration of adsorbed VOC-odor on aerosol surface (kg m^{-3})
q_e	equilibrium adsorbed phase concentration (kg kg^{-1})
q^*	dimensionless variable of q
$\hat{q}^*(s)$	Laplace-transformed q^*
s	Laplace variable
$\mathrm{sd}_\tau, \mathrm{sd}_k$	standard deviation of gamma distributions for τ and K
t	time (h)
$\bar{t}$	nominal mean residence time (h)
T	dimensionless variable of t
$U(t)$	unit step function
v	air velocity (m s^{-1})
V	dimensionless variable of v
V_c	air volume occupied by complete mixing (m^3)
V_i	air volume occupied by incomplete mixing (m^3)
V_p	air volume occupied by piston flow (m^3)
V_T	total volume in the system (m^3)
x	mean direction of airflow (m)
X	dimensionless variable of x
Greeks	
α_τ, β_τ	shape and scale parameters of gamma distribution of τ

α_k, β_k	shape and scale parameters of gamma distribution of K
γ	gamma distribution
ρ	aerosol density (kg m^{-3})
θ	mixing volume factor I
θ_m	surface volumetric moisture content of aerosol (v/v)
τ	dimensionless residence time of airflow
$\bar{\tau}$	mean of gamma distribution of τ
μ	mixing efficiency
η	mixing volume factor II
ξ	dummy variable of integration in gamma function
$\Gamma(\cdot)$	gamma function

Conventional approaches to deal with the airflow mixing problem often assume that mixing patterns are homogeneous or can be represented as an equivalent complete mixing mechanism so that every mixing process can be described in a deterministic manner. It is evident however that this assumption is not always valid. Barber and Ogilvie [7] suggested that departure from complete mixing might be caused by the formation of multiple flow regions within the airspace or short-circuiting of supply air to exhaust outlet. A work by Chen et al. [8] regarding the methods to measure dust production and deposition rates in buildings indicated that the assumption of complete mixing was not valid during tests. Their experimental data showed that tanks-in-series flow, i.e., different flow regions behaving as a number of mixed tanks connected in series dominated the overall mixing process within the ventilated airspace. Their work also suggested that a more complicated multi-zone mixing model might be needed to account for heterogeneous mixing to better understand the behavior of dust local transport mechanisms.

Simulation models for the transport of VOC-odor in ventilated animal housing are important tools for testing our understanding of transport phenomena and for designing management strategies for creating a healthy microclimate for workers and animals. From a management perspective, knowing both when a VOC-odor will arrive at a given location in a ventilated airspace and how much of the air exchange rate purges the VOC-odor are of extreme importance.

Assessment of indoor air quality issues regarding odor/VOC-odor transport in ventilated animal housing requires the consideration of different control strategies and various air pollution control options. The decision-making process leading to the optimal control strategy now relies heavily on quantitative computer models of airflow and odor/VOC-odor transport in ventilated airspace. These approaches in turn call for model development of the pertinent physicochemical and biological processes. Thus, we need a detailed understanding of the phenomena controlling the dynamic transport processes of VOC-odor and we must be able to rely on quantitative models that are able to capture the main features of these processes.

For VOC-odor, a key process to include in any transport model is adsorption. At the particle scale, the governing processes of kinetic adsorption/desorption are complex and poorly understood. A variety of processes is related to the complexity and heterogeneity of the interaction between VOC-odor and ambient aerosol profile. In addition, due to multiple airflow regions of heterogeneous mixing and stagnant airflow, large-scale heterogeneity can create physical nonequilibrium that may be observed in the transport of adsorbed and nonadsorbed VOC-odors.

Fig. 1 illustrates a reactive VOC-odor moving through a medium of ambient aerosol or bioaerosol in the mean airflow direction x. Sorption reactions often affect the movement and fate of VOC-odor in a highly dusty livestock building environment (Fig. 1(A)). The sorption of

VOC-odor on airborne dust is dominated by the behavior of the interactions among VOC-odor, airborne dust, and dust-borne VOC-odor [5]. The mechanistic function of airborne dust in the uptake of VOC-odor may be partitioning and/or adsorption (Fig. 1(B)). The ventilated airspace is composed of a heterogeneous mixing airflow field and a continuum of sorbing surfaces of ambient aerosol/bioaerosol (Fig. 1(C)). The VOC-odor can be sorbed either instantaneously or time-dependently onto a fraction of the surface of airborne dust during transport. The term "surface" here means a sorbing domain or portion of the sorbing site of airborne dust envisioned as a fraction having uniform local sorption properties.

The sorption mechanisms at each surface are presumed to be either a diffusion controlled process or a combination of diffusion and sorption kinetics. A nonequilibrium model has to have a sufficient capability to represent a variety of adsorption/desorption and transport mechanisms including sorption rate limitations, first-order approximations of diffusion and physical nonequilibrium. A stochastic approach may be incorporated to analyze a given heterogeneity in air mixing, in size, shape and composition of ambient aerosol in that the airflow residence time,

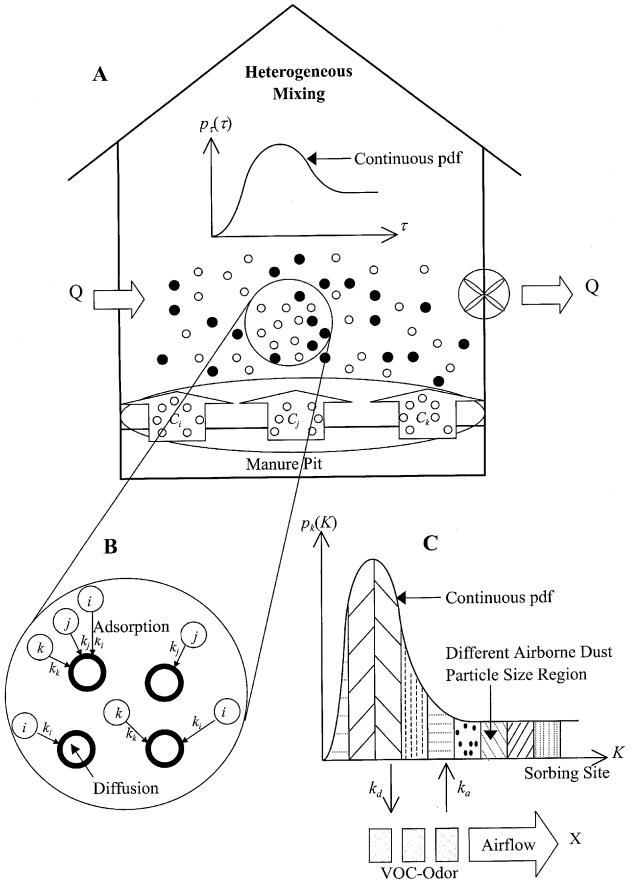

Fig. 1. An integrated scheme showing mixing/adsorption heterogeneity in a ventilated animal unit: (A) VOC-odor (○) and airborne dust (●) mixture in a ventilated airspace where the heterogeneous air mixing is described by a continuous pdf of residence time distribution, (B) adsorption and diffusion behaviors between VOC-odor and airborne dust where the mechanistic function of airborne dust in uptake of VOC-odor may be partitioning and/or adsorption, and (C) VOC-odor in the mean airflow direction and sorption in airborne dust medium with different particle sizes described by a continuous pdf of adsorption rate coefficient.

sorption equilibrium constant, first-order mass transfer rate constant and/or diffusion coefficient are continuously distributed.

The objective of this paper is to generalize a dynamic transport model of VOC-odor in a ventilated airspace under heterogeneity of both air mixing and adsorption kinetics between VOC-odor and ambient aerosol. The model incorporates with a probability density function (pdf) describing both residence time of airflow and adsorption rate parameters in the first-order mass transfer process approximated at a local scale.

In this paper we present a transfer function modeling technique [9] to explain the dynamic response between adsorbed- and gas-phase VOC-odor in heterogeneous mixing/adsorption ventilated airspace. The determination of the transfer function of a system, i.e., the determination of a dynamic input–output model that can show the effect on the output of a system subject to any given series of inputs. Transfer function model building is important because it is only when the dynamic characteristics of a system are understood that manipulation and control of the system is possible. Deterministic perturbations of the boundary inputs such as step and impulse response functions were used for testing the dynamic behavior of the transfer function models.

2. Model and solution technique

2.1. Transfer function modeling

Two model simplifications are inherent in our analysis: (1) neglect of local dispersion and molecular diffusion processes, and (2) neglect of deposition of ambient aerosol and adsorbed VOC-odor.

Neglect of dispersion processes. This simplification represents a reasonable approximation, since only within a few airflow regions where airborne dust concentration changes rapidly result in dispersion processes [8,11]. By excluding such regions, any dispersion effect can be safely neglected. Reliable estimates of the dispersivity that may be scale-dependent, however, are very difficult to obtain. The dispersive effect is also characterized by other limitations. Liu et al. [12] and Hoff and Bundy [13] pointed out that the theoretical foundation for the dispersive effect in multiple airflow regions is not sound for systems other than an air jet with turbulent or laminar flow. The model assumes that molecular diffusion is negligible indicating the existing gaseous or particulate contaminates and air is identical and both are related to the distribution of air velocities. This condition, however, is not that restrictive since molecular diffusion is negligible compared with mechanical dispersion in most situations, especially in large-scale systems.

Neglect of solid-phase deposition. A simple criterion to ascertain the validity of this approximation is to show that the product of the deposition rate coefficient and the average residence time is not considerably larger than unity [5]. A theoretical study by Liao et al. [5] shows that the ratios between adsorption and deposition rates for two different aerosol profiles of 2 and 8 μm geometric mean diameters in a ventilated airspace have the magnitudes ranged from about 10^1 to 10^2. Thus, a relative comparison with adsorption, deposition reflects an insignificant contribution to the transport mechanisms.

Although local dispersion and molecular diffusion have been omitted, the macroscopic dispersive effects retained through the ensemble approaches are described later for random velocity field and its heterogeneous mixing patterns.

A one-dimensional form of the advection–dispersion–reaction equation incorporating sorption equilibrium and rate expression [10] was employed to describe the dynamic transport of VOC-odor in heterogeneous mixing/sorption ventilated airspace. The transport of VOC-odor with

mixing/sorption kinetics heterogeneity may be characterized by coupling the dynamics of the time evolution of VOC-odor concentration $c(x,t)$ (kg m^{-3}) and concentration of adsorbed VOC-odor (or dust-borne VOC-odor) $q(x,t)$ (kg kg^{-1}) on the ambient aerosol surface as

$$\frac{\partial c}{\partial t} = -v(x)\frac{\partial c}{\partial x} - \frac{\rho}{\theta_{\mathrm{m}}}\left[\frac{\partial q_{\mathrm{e}}}{\partial c}\frac{\partial c}{\partial t} - \frac{\partial q}{\partial t}\right], \tag{1}$$

$$\frac{\partial q}{\partial t} = k(k_d c - q), \tag{2}$$

the second term of right-hand side of Eq. (1) is an equilibrium adsorption isotherm, whereas the third term is a first-order mass transfer approximation that can also be expressed as Eq. (2). In Eqs. (1) and (2), v is the air velocity (m s^{-1}), ρ is the aerosol density (kg m^{-3}), θ_{m} is the surface volumetric moisture content of aerosol (%, v/v), q_{e} is the equilibrium adsorbed phase concentration (kg kg^{-1}), k is the adsorption rate coefficient (h^{-1}), k_d is the linear partitioning coefficient between gas and solid phases at sorption equilibrium (m^3 kg^{-1}), and $c(x,t)$ and $q(x,t)$ are both functions of the mean airflow direction x and the time t.

We adopted the commonly used first-order mass transfer approximation (Eq. (2)) at the local scale to simplify the complications of the aerosol geometric specification required in the diffusion formulation. The rate coefficient in Eq. (2) inherently lumps all the local geometric influences as if a diffusion mechanism is dominant. A first-order mass transfer or a diffusion process presented in Eq. (2) can generally use a density function to describe the process of mass sorption/desorption between the mixing airspace and the sorbing surfaces. The adsorbed VOC-odor, $q(x,t)$, can then be described by a convolution integral as

$$\frac{\rho}{\theta_{\mathrm{m}}}q(x,t) = \int_0^\infty c(x,t')h(t-t')\,\mathrm{d}t', \tag{3}$$

where $h(t)$ is a density function.

We introduced the dimensionless variables of $X = x/L_0$, $T = t/\bar{t}$, $C^* = c/C_0$, $q^* = \rho q/\theta_{\mathrm{m}}C_0$, $V = v\bar{t}/L_0$, $K_{\mathrm{D}} = k_d\rho/\theta_{\mathrm{m}}$, and associated with a linear isotherm of $q_{\mathrm{e}} = k_d c$ to nondimensionalize Eqs. (1) and (3). Eqs. (1) and (3) can then be reduced to the following dimensionless forms as:

$$\frac{\partial C^*}{\partial T}(1+K_{\mathrm{D}}) = -V(X)\frac{\partial C^*}{\partial X} - \frac{\partial q^*}{\partial T} \tag{4}$$

and

$$q^*(X,T) = \int_0^\infty C^*(X,T')h(T-T')\,\mathrm{d}T', \tag{5}$$

where the reference parameters $L_0, \bar{t}$, and C_0 are the distance from face of outlet, nominal mean residence time of airflow ($\bar{t} = V_{\mathrm{T}}/Q$), where V_{T} (m^3) is the total volume in the system and Q (m^3 s^{-1}) is the volumetric airflow rate), and input concentration, respectively.

Eqs. (4) and (5) can be solved in the Laplace domain under zero initial conditions of C^* and q^*, and a constant input of unit mass at $X = 0$ as $C^*(T, X = 0) = U(T)$ where $U(T)$ is a unit step function defined from the positive direction

$$\hat{C}^*(s) = s^{-1}\exp\left[-s\tau\left(1+K_{\mathrm{D}}+\hat{h}(s)\right)\right] \tag{6}$$

and

$$\hat{h}(s) = \frac{\hat{q}^*(s)}{\hat{C}^*(s)}, \tag{7}$$

where $\hat{h}(s)$ is referred to as the transfer function for the rate-limiting processes and s is the Laplace variable. In Eq. (6), τ is the residence time of airflow that was released at the inlet $X = 0$ and reached the outlet $X = 1$ with air velocity V under no influence of any rate-limiting process and has the form as,

$$\tau = \int_0^1 \frac{\mathrm{d}X}{V(X)}, \tag{8}$$

where air velocity V may be envisioned in the microscopic point of view as a mean projection of the three-dimensionally oriented velocity along the gas-phase trajectory onto the X-coordinate.

The dimensionless form of the first-order mass transfer approximation in Eq. (2) can be written as

$$\frac{\partial q^*}{\partial T} = K(K_{\mathrm{D}}C^* - q^*), \tag{9}$$

where $K = k\bar{t}$ is the dimensionless rate coefficient. Taking the Laplace transform of Eq. (9) gives

$$\hat{h}(s) = \frac{\hat{q}^*(s)}{\hat{C}^*(s)} = \frac{KK_{\mathrm{D}}}{s + K}. \tag{10}$$

2.2. Statistical ensemble solution

Liao and Liang [14] developed a model called multiple airflow regions gamma model (MARGM) that is based on a continuous distribution of residence time for predicting the mixing behavior in a ventilated airspace. The MARGM takes the form of a two-parameter gamma distribution and accounts for different mixing patterns such as incomplete, complete–incomplete, incomplete–complete–piston flow, and various combinations of the above types. The applicability of MARGM was tested by several case studies. Simulation results showed that heterogeneous mixing models gave a better fit than a homogeneous one, suggesting that the candidate pdf for the residence time of airflow (τ), $p_\tau(\tau)$, is a two-parameter gamma distribution.

The gamma distribution is a distribution of the Pearson's Type III in statistics. The unique feature of the gamma distribution is that one end of the distribution is bound to a fixed value, whereas the other end is distributed over a large scale of variate. The overall shape of the gamma distribution is not balanced as a normal distribution. The other reason to utilize the gamma distribution is that this approach may reduce the mathematical terms in the analytical solution. The gamma pdf of τ is given by

$$p_\tau(\tau; X = 1) \equiv \gamma(\tau; \alpha_\tau, \beta_\tau) = \frac{\beta_\tau^{-\alpha_\tau}\tau^{\alpha_\tau - 1}}{\Gamma(\alpha_\tau)} \exp\left(-\frac{\tau}{\beta_\tau}\right), \tag{11}$$

where α_τ (the shape parameter) and β_τ (the scale parameter) are positive parameters, $\Gamma(\alpha_\tau)$ is the gamma function as $\Gamma(\alpha_\tau) = \int_0^\infty \xi^{\alpha_\tau - 1}\exp(-\xi)\,\mathrm{d}\xi$, where ξ is a dummy variable of integration, and $p_\tau(\tau; X = 1)\,\mathrm{d}\tau$ is the probability for a VOC-odor to have residence time between τ and $\mathrm{d}\tau$ before exiting the system at $X = 1$. It should be noted that the mean residence time in dimensionless form is always unity. With the gamma model, the mean and standard deviation of the distribution are $\bar{\tau} = \alpha_\tau\beta_\tau$ and $\mathrm{sd}_\tau = \alpha_\tau^{1/2}\beta_\tau$, respectively.

The following relations give the shape and scale parameters of α_τ and β_τ in the MARGM [14]

$$\alpha_\tau = \begin{cases} \dfrac{V_T}{V_p + V_c + \mu V_i} = \dfrac{1}{\frac{1}{\theta} + \mu\left(1 - \frac{1}{\theta}\right)}, & \mu \geqslant 0.5, \\ \dfrac{V_T}{V_p + V_c + (1-\mu)V_i} = \dfrac{1}{\frac{1}{\theta} + (1-\mu)\left(1 - \frac{1}{\theta}\right)}, & \mu \leqslant 0.5, \end{cases} \tag{12}$$

$$\beta_\tau = \frac{1}{\alpha_\tau\left(\frac{V_T}{V_c + \mu V_i}\right)} = \frac{1}{\alpha_\tau}\left(\frac{1}{\eta\theta} + \mu - \frac{\mu}{\theta}\right) \tag{13}$$

in which

$$\theta = \frac{V_T}{V_c + V_p} \tag{14}$$

and

$$\eta = \frac{V_T}{\theta V_c}, \tag{15}$$

where V_c, V_p and V_i represent the air volumes occupied by complete mixing, piston flow and incomplete mixing, respectively; $V_T = V_c + V_p + V_i$ is the total volume in the system; is the mixing efficiency; θ and η may be referred to as the mixing volume factors I and II, respectively. The mixing efficiency μ is defined to describe the extent of heterogeneous mixing resulting from factors other than molecular diffusion in that $\mu = 1$ for complete mixing, $\mu = 0$ for piston flow, and heterogeneous mixing is characterized by $0 < \mu < 1$.

In view of Eq. (9), the dimensionless equilibrium partition coefficient (K_D) and the adsorption rate constant (K) are lumped parameters to characterize some variations in VOC-odor components and within the ambient aerosol size fraction distribution that may cause considerable fluctuations of the local rate process as the VOC-odor diffusion through or adsorbs onto the aerosol surface. It is reasonable to treat both K_D and K as randomly distributed variables.

Based on the concept of linear free-energy relationships (LFERs) [10,15], the logarithms of equilibrium constants associated with changes in reactant structure in parallel reactions should be linearly related to each other and are often negatively correlated. In this study, we employed the LFERs concept to approximate the relationship between the two log-transformed parameters, $\log K_D$ and $\log K$, (i.e., linear $\log K_D \sim \log K$) and has the form as,

$$K_D = aK^{-b}, \tag{16}$$

where a and b are two positive constants. Two extreme cases of correlation are represented by Eq. (16) as b takes zero or nonzero values. If $b = 0$, a completely independent relationship exists between K_D and K; whereas any nonzero value of b gives a perfect correlation between K_D and K. Therefore, a perfect correlation would simplify the bivariate pdf ($p_{dk}(K_D; K)$) to being univariate. The resulting univariate pdf can be represented either by the pdf of $K_D(p_d(K_D))$ or by the pdf of $K(p_k(K))$. In this work, we assume K_D is constant at all adsorption surfaces, thus, a pdf of $K(p_k(K))$ is used to characterize the variations.

Yeh et al. [16] recently developed a mathematical model to predict the adsorption rate constant of VOC-odor on the ambient airborne dust based on a gamma distribution of adsorption rate coefficients and with the consideration of a distributed Fick's diffusion model as experimental test data. Results showed that the model had successfully fit the test data using a gamma distribution of rate coefficients. The use of a gamma distribution of rate constants is to assume a continuum of "physical lumps" in an ambient aerosol profile with each "lump" being characterized by its own adsorption rate constant.

The gamma pdf of K is given by

$$p_k(K) \equiv \gamma(K;\alpha_k,\beta_k) = \frac{\beta_k^{-\alpha_k} K^{\alpha_k-1}}{\Gamma(\alpha_k)} \exp\left(-\frac{K}{\beta_k}\right), \tag{17}$$

where α_k is the shape parameter, β_k is the scale parameter, and $\Gamma(\alpha_k)$ is the gamma function. The mean and standard deviation of the distribution are $\bar{K} = \alpha_k\beta_k$ and $\mathrm{sd}_k = \alpha_k^{1/2}\beta_k$, respectively.

Other pdfs may be also available. For example, local VOC-odor diffusion and adsorption rate coefficients have been related to ambient aerosol particle size that is typically considered to be a log-normal distribution [4,5], suggesting that the log-normal distribution would also be a potential candidate to describe the mass transfer rate distribution. The primary interest of this research, however, is not on the attributions of different pdfs.

By knowing the pdfs of τ and K as shown in Eqs. (11) and (17), the expected output concentration and mean transfer function for the first-order mass transfer can be calculated through Eqs. (6) and (10), respectively, by taking a mathematical expectation operator $E[\cdot]$ in the Laplace domain as

$$\hat{C}(X=1,s) = E\left[\hat{C}^*(s)\right] = \int_0^\infty \hat{C}^*(s) p_\tau(\tau, X=1)\,\mathrm{d}\tau \tag{18}$$

and

$$\hat{H}(s) = E\left[\hat{h}(s)\right] = \int_0^\infty \frac{aK^{1-b}}{s+K} p_k(K)\,\mathrm{d}K, \tag{19}$$

By substituting Eqs. (11), (16), and (17) into Eqs. (18) and (19), respectively, the final expression is

$$\hat{C}(X=1,s) = \int_0^\infty \int_0^\infty s^{-1} \exp\left[-s\tau\left(1 + aK^{-b} + \hat{H}(s)\right)\right] \gamma(K;\alpha_k,\beta_k)\gamma(\tau;\alpha_\tau,\beta_\tau)\,\mathrm{d}K\,\mathrm{d}\tau, \tag{20}$$

where $\hat{H}(s)$ has the following forms as:

$$\hat{H}(s) = \int_0^\infty \frac{aK^{1-b}}{s+K} \gamma(K;\alpha_k,\beta_k)\,\mathrm{d}K, \tag{21}$$

Eq. (21) reveals that ensemble transfer function includes four parameters: two common constants of a and b and two specific parameters of α_k and β_k. The four parameters, however, may be reduced to three after subjecting the constraint of the sample-averaged K_D as

$$E[K_\mathrm{D}] = \bar{K}_\mathrm{D} = aE[K^{-b}] = a\beta_k^b \frac{\Gamma(\alpha_k - b)}{\Gamma(\alpha_k)}, \tag{22}$$

where $E[K^{-b}]$ is the bth moment in the statistical sense. Eq. (22) indicates that whenever three of the four parameters are chosen, the fourth is automatically determined by Eq. (22).

The inverse Laplace transform of $\hat{C}(X=1,s)$ in Eq. (20) provides an expected concentration output across the exit plane at $X=1$ under the corresponding unit step input boundary conditions in a ventilation system. A Dirac (impulse) input boundary condition was also employed in the model simulation in that $\hat{C}^*(s)$ in Eq. (6) became

$$\hat{C}^*(s) = \exp\left[-s\tau\left(1 + K_\mathrm{D} + \hat{h}(s)\right)\right]. \tag{23}$$

Fig. 2 illustrates a conceptual algorithm showing the system process, system transfer function, governing equations and computational procedures.

2.3. Numerical issues

Analytical inversion of Eq. (20) may be possible yet would probably lead to complex integrals. Therefore, numerical inversion to obtain the solution is adopted. Numerous algorithms that have been successfully applied to numerically invert the Laplace transformed analytical solution include the Stehfest algorithm [17], the Talbot algorithm [18], the Crump algorithm [19] and the de Hoog et al. algorithm [20]. In the present research, we adopted the de Hoog et al. algorithm to perform the inversion of Eq. (20). The de Hoog et al. algorithm provides a good accuracy for a wide variety of functions and it also performs reasonably well in the neighborhood of a discontinuity (i.e., the shape front). The Laplace transform parameter has to be declared as a complex variable in computation when the de Hoog et al. algorithm is used.

A FORTRAN subroutine DINLAP/INLAP provided by IMSL Subroutines Library [21] based on the de Hoog et al. algorithm is employed to perform the Laplace transform. (The program is available upon request from the authors.)

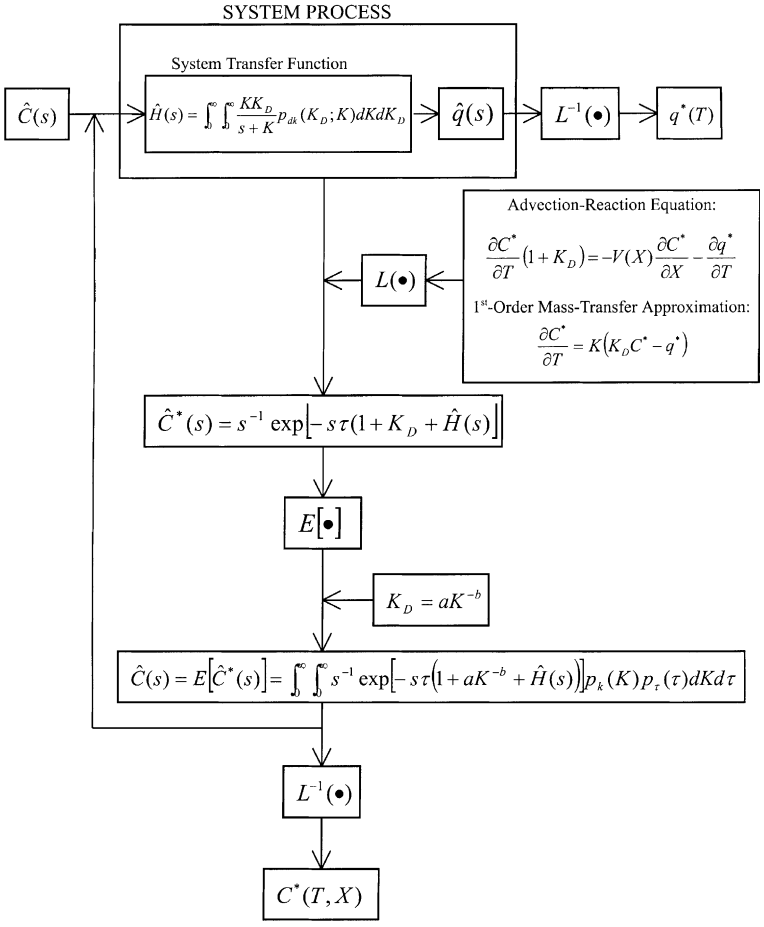

Fig. 2. Schematic illustration of a conceptual algorithm showing the system transport process, system transfer function, governing equations, and computational procedures in the case of a boundary unit step response function.

3. Results and discussion

The effects of mean adsorption rate coefficient ($\bar{K}$), mean residence time of airflow ($\bar{\tau}$), mean partitioning coefficient ($\bar{K}_D$), coefficient of variation (CV) for K and τ(CV_k and CV_τ) on VOC-odor transport were performed systematically as seven cases based on the input parameters given in Table 1. In this study, we employed three different mixing patterns including incomplete mixing, complete–incomplete mixing, and complete–incomplete–piston flow.

Simulation results in the cases of impulse and unit step inputs boundary conditions are presented in Figs. 3–6. Table 2 gives the calculated peak concentrations and the time to peak concentrations, whereas Table 3 lists the calculated equilibrium concentrations and the times to 99% equilibrium concentration. Generally, the equilibrium concentrations are higher than the peak concentrations at the same simulation conditions (Tables 2 and 3).

Comparison between models of simulated output dynamics from the mixing/adsorption heterogeneity under different $\bar{K}$ values at different $\bar{\tau}$ of 1 and 4 is illustrated in Fig. 3 (for cases 1 and 2). Fig. 3 shows that the peak and the equilibrium concentrations of the output curves decreased as the $\bar{K}$ values increased from 4 to 100, indicating high dependence upon the relative adsorption rate coefficient during the transport process.

When the $\bar{K}$ value is low, sorption is generally slower than transport and nonequilibrium conditions are present. This implies that most VOC-odor bypass a continuum of adsorption surfaces of airborne dust, resulting in a sharp peak and a very small amount of sorbed VOC-odor to produce a flattened curve tail (Fig. 3(A) and (B)). Nonequilibrium conditions are less severe in the high $\bar{K}$ value case in that most VOC-odors have sufficient time to diffuse to or react with the continuum of adsorption surfaces of ambient aerosol and thus result in a wider peak.

Table 1
Input parameter used for simulation of VOC-odour transport under mixing/adsorption heterogeneity

Mixing pattern	Cases	$\bar{K}$	α_k	β_k	CV_k	α_τ	β_τ	CV_τ	a	b	$\bar{K}_D$	μ[a]
Incomplete[b]	1a	4	2	2	0.707	1	1	1	2	1	4	0.502
	1b	10	5	2	0.707	1	1	1	2	1	1	0.502
	1c	40	20	2	0.707	1	1	1	2	1	0.211	0.502
	1d	100	50	2	0.707	1	1	1	2	1	0.082	0.502
	2a	4	2	2	0.707	4	1	1	2	1	4	0.502
	2b	10	5	2	0.707	4	1	1	2	1	1	0.502
	2c	40	20	2	0.707	4	1	1	2	1	0.211	0.502
	2d	100	50	2	0.707	4	1	1	2	1	0.082	0.502
	3a	4	2	2	0.707	2	1	1	2	1	4	0.502
	3b	4	20	0.2	2.236	2	1	1	2	1	0.021	0.502
	4a	0.4	2	0.2	2.236	2	2	0.707	2	1	0.4	0.502
	4b	1	2	0.5	1.414	2	2	0.707	2	1	1	0.502
	4c	10	2	5	0.447	2	2	0.707	2	1	10	0.502
	4d	40	2	20	0.224	2	2	0.707	2	1	40	0.502
	4e	100	2	50	0.141	2	2	0.707	2	1	100	0.502
Complete–Incomplete[b]	5a	10	2	5	0.447	2	0.2	2.236	2	1	10	0.671
	5b	10	2	5	0.447	0.2	2	0.707	2	1	10	0.671
	6a	10	2	5	0.447	2	2	0.707	2	1	10	0.671
	6b	10	2	5	0.447	5	0.8	1.124	2	1	10	0.671
Complete–Incomplete–Piston[b]	7a	4	2	2	0.707	2	2	0.707	1	0	1	0.312
	7b	4	2	2	0.707	2	2	0.707	10	0	10	0.312
	7c	4	2	2	0.707	2	2	0.707	2	0.1	1.07	0.312
	7d	4	2	2	0.707	2	2	0.707	2	1	4	0.312

[a] Values are determined based on Eqs. (12)–(15).
[b] Mixing pattern is determined based on the relations of $V_T = V_c + V_p + V_i$ and Eq. (11).

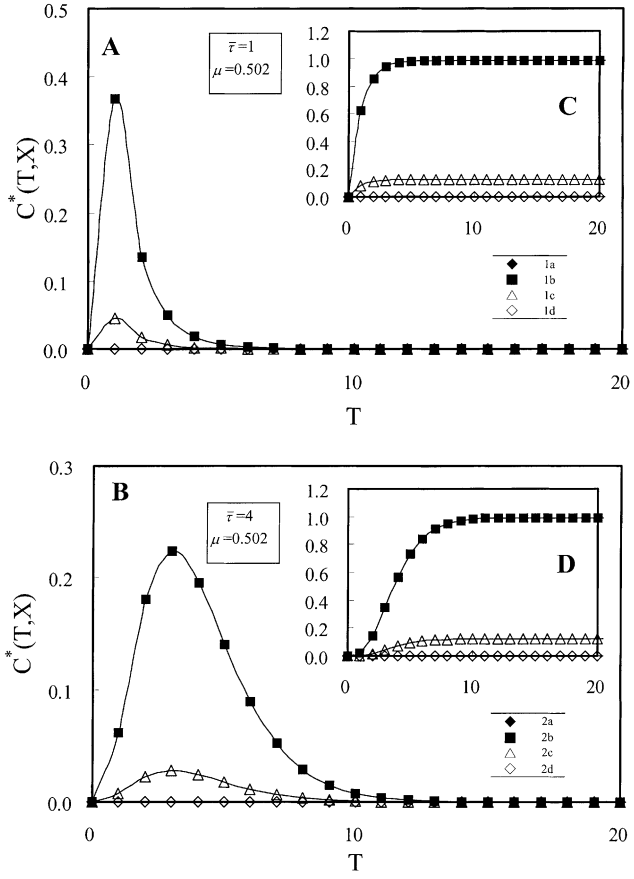

Fig. 3. Effect of mean adsorption rate coefficient ($\bar{K}$) on output VOC-odor concentration in an incomplete mixing regime ($\mu = 0.502$) for impulse (A) and (B) and unit step (C) and (D) response functions based on cases 1 and 2.

The model less affected by $\bar{K}$ further indicates the complimentary effect of assuming a range of sorption surfaces. As seen from the current simulations where the same $CV_k = 0.707$ was used for K in both cases 1 and 2, substantial deviation between output curves still exists, indicating sorption surface heterogeneity. The high dependence on $\bar{K}$ may also imply that this model can be highly air velocity-dependent.

The effects of different CV_k and K at $\bar{\tau}$ of 1 and 4 are shown in Fig. 4 (for cases 3 and 4) in that Fig. 4(A) and (C) have the same $\bar{K}$ but different CV_k, whereas the different $\bar{K}$ and CV_k for Fig. 4(B) and (D). Theoretically, when the value of the CV_k tends to zero, it represents homogeneous sorption behavior. Fig. 4(B) shows that an apparently higher variability of sorption rate would spread VOC-odor peak more significantly. Fig. 4 also indicates that the peak spreading is limited in the model since the increase of the sorption rate variability means that the rate deviation increases between the distinct surfaces. That is to say, the higher $\bar{K}$ values at lower CV_k result in a distributed instead of a more sharpened peak.

Table 2 indicates that in case 4, the predicted peak concentration varied by up to one order of magnitude as the order of magnitude of $\bar{K}$ values increased from $<10^1$ to 10^2, but not for the unit step response function presented in Table 3.

Fig. 5 (for cases 5 and 7) compares the influence of different $\bar{\tau}$ and CV_τ values on the simulation results. When the $\bar{\tau}$ values are high, the peak and the equilibrium concentrations are generally higher and the times to the peak and the equilibrium concentrations are longer as well (Tables 2

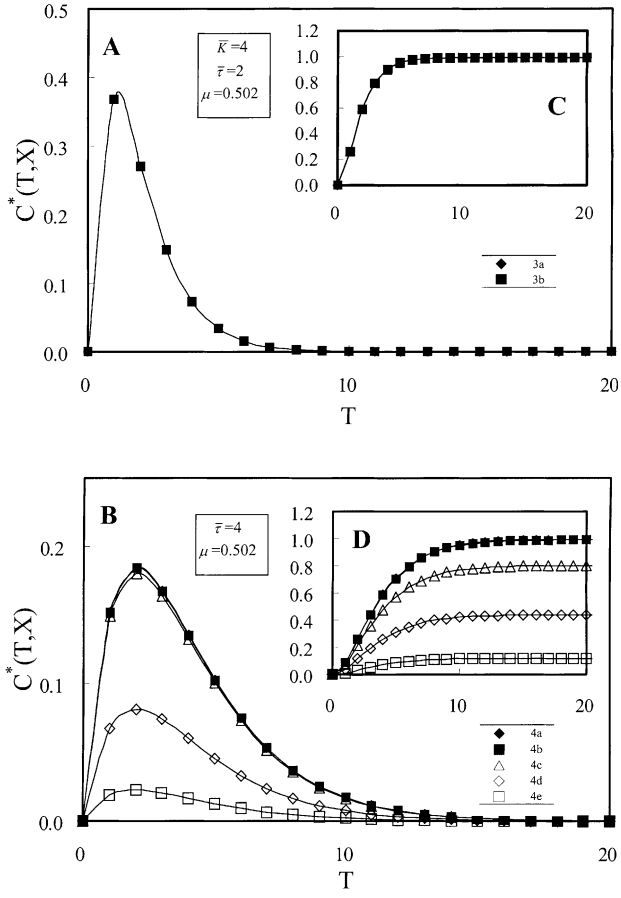

Fig. 4. Effect of coefficient of variation of K (CV_k) on output VOC-odor concentration in an incomplete mixing regime ($\mu = 0.502$) for impulse (A) and (B) and unit step (C) and (D) response functions based on cases 3 and 4.

and 3). At large residence time ($\bar{\tau}$) means at low airflow rate as well, the VOC-odor remains longer in the ventilated airspace, indicating that there is more time for diffusion into airborne dust. This causes the differences between the output curves at different $\bar{\tau}$ values. The shape of the output curve is then determined by the ratio of airflow rate and adsorption rate. Fig. 5(C) shows that higher CV_τ values would spread the VOC-odor peak more significantly, indicating heterogeneous mixing behavior. In the present study, the form of dispersion is not included in the model. Dispersion, however, mainly affects the initial part of the output curve and becomes less significant when VOC-odor diffusion into airborne dust becomes more important.

The influence of different $\bar{K}_D$ values on the simulation results is illustrated in Fig. 6 (for case 7). As was shown in Fig. 6, the simulation results indicate that $\bar{K}_D$ values have less influence on output profiles. An increase in $\bar{K}_D$ increases the peak as well as the concentration level in the output curves. Therefore, when a pdf of K is incorporated into the model, a change in $\bar{K}_D$ would not significantly change the model predictions. This indicates that the present model, with no correlation between K_D and K, may approximate the cases where K_D and K are not strictly correlated (as in Eq. (16)).

In summary, modeling the VOC-odor transport in a heterogeneous mixing ventilated airspace with heterogeneous adsorption of VOC-odor on the ambient aerosol surface has proven challenging because the specific processes and response mechanisms associated with particular physical domain changes are unknown. The ultimate goal for many building microclimate

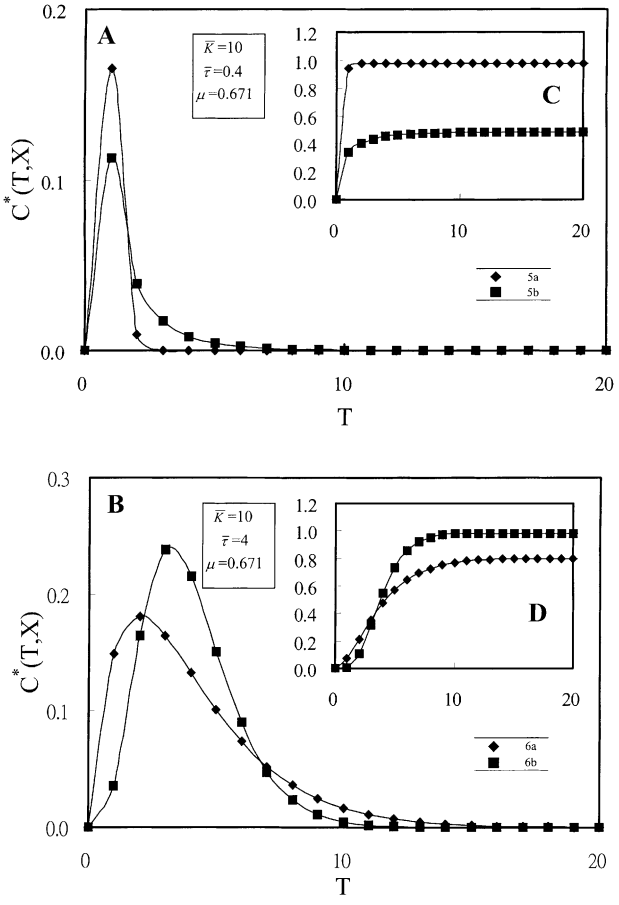

Fig. 5. Effect of coefficient of variation of τ (CV_τ) and mean residence time ($\bar{\tau}$) on output VOC-odor concentration in a complete–incomplete mixing regime ($\mu = 0.671$) for impulse (A) and (B) and unit step (C) and (D) response functions based on cases 5 and 6.

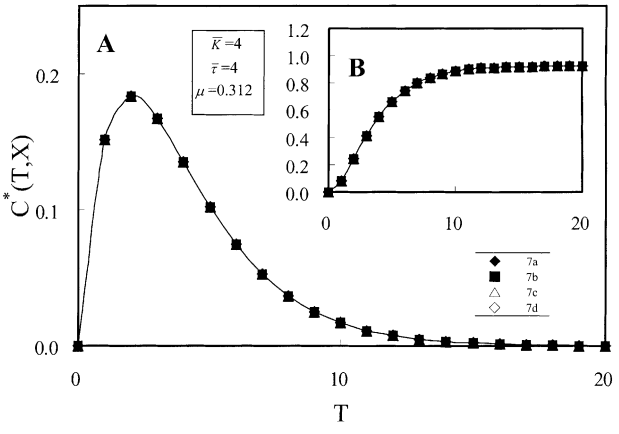

Fig. 6. Effect of mean linear partitioning coefficient ($\bar{K}_D$) on output VOC-odor concentration in a complete–incomplete-piston flow mixing regime ($\mu = 0.312$) for impulse (A) and unit step (B) response functions based on case 7.

Table 2
Calculated peak concentrations and the time to peak concentrations in the case of impulse response function

Cases	Peak concentration (–)	Time to peak concentration (–)
1a	0.368	1
1b	0.367	1
1c	0.046	1
1d	3.81×10^{-13}	1
2a	0.224	3
2b	0.223	3
2c	0.028	3
2d	1.83×10^{-13}	3
3a	0.368	1
3b	0.367	1
4a	0.185	2
4b	0.184	2
4c	0.181	2
4d	0.081	2
4e	0.022	2
5a	0.166	1
5b	0.113	1
6a	0.181	2
6b	0.238	3
7a	0.184	2
7b	0.184	2
7c	0.184	2
7d	0.184	2

Table 3
Calculated equilibrium concentrations and the time to 99% equilibrium concentrations in the case of step response function

Cases	Equilibrium concentration (–)	Time to equilibrium concentration (–)
1a	0.992	5
1b	0.991	5
1c	0.124	5
1d	1.13×10^{-24}	5
2a	0.993	11
2b	0.992	11
2c	0.124	11
2d	8.45×10^{-13}	11
3a	0.993	8
3b	0.993	8
4a	0.994	11
4b	0.989	11
4c	0.797	11
4d	0.438	11
4e	0.121	11
5a	0.979	2
5b	0.483	2
6a	0.797	11
6b	0.983	11
7a	0.902	11
7b	0.902	11
7c	0.902	11
7d	0.902	11

designers is the identification and understanding of these controlling processes and their subsequent incorporation into reliable predictive models that could be used for addressing practical indoor air quality management problems.

Results from this study demonstrate that the complexity of factors affecting VOC-odor concentrations and air mixing patterns often reflect differences in aspect in a predictable way, indicating the overall VOC-odor transport processes in a ventilation system are almost certainty nonlinear with respect to both space and time, and the present study was not designed to formally test the null hypothesis that VOC-odor transport is in a linear fashion. Instead, the goal of this study was to evaluate the extent to which a parsimonious linear transfer function technique could approximate the transient response of a ventilated airspace with mixing/adsorption heterogeneity to describe VOC-odor transport.

The development, testing, and application of transfer function approach in our proposed form does not derive from an a priori assumption that VOC-odor transport in building airflow systems are inherently linear, but from the practical view that seeks to extract the maximum usefulness from linear methodology before accepting the complexities attending nonlinear approaches. Several real advantages of transfer function technique over nonlinear approaches may include: (1) computational simplicity, (2) ease of calibration for well-characterized systems, and (3) capability of extrapolating to other uncharacterized systems.

We also acknowledge that computational fluid dynamics (CFD) is increasingly being used by engineers for building microclimate design, because it provides very detailed information that is effectively unobtainable by other means. Because of its fundamental nature, CFD is probably the most adaptable of all the techniques for studying ventilation, e.g., as a means of flow visualization. It can certainly be applied to a very wide range of diverse problems both for research and design. It does, however, have fundamental limitations, the main ones being that its accuracy is ultimately limited by uncertainties in specifying boundary conditions and that it cannot predict instantaneous properties of turbulence. In the long run the latter limitation may be reduced, but the former will always remain. Limitations that are more related to the physics are the empiricisms employed for the coefficients in the equations.

While it is certainly true that these advantages of transfer function technique are not nearly as important today as they were two decades ago because of advances in development of digital computers, it needs to be reemphasized that transfer function technique of the form proposed does not suffer from so-called ''overparameterization'' associated with many CFD models (e.g., κ–ε model). Philosophically, it can be argued that parsimony is a legitimate modeling objective and additional model complexity (often in the form of nonlinearity) should only be advocated if it can be shown to significantly reduce uncertainties normally attributed to random system or measurement errors.

Finally, while the results of the present study are generally supportive of the transfer function approach, a more rigorous test of the methodology would include application the CFD modeling technique to an even broader array of design of building environments in order to determine whether employed model might be appropriate. In the case of the transfer function technique, it is hoped that additional experimental data with well-documented test information can be used to confirm or reject the overall applicability of a comparable transfer function approach to modeling indoor air quality problems.

4. Conclusions

The transport of VOC-odor in a ventilated airspace is inherently complex for a heterogeneous mixing/adsorption system that is characterized by a wide particle size distribution, particle surface, heterogeneous physicochemical–biological composition on particle surface, and various mixing patterns. Any mathematical model, assumption may bias results. The present model assumes isotherm linearity. The concept of sorption equilibrium proposes that, given a sufficient

time, a predictable ratio of gaseous-phase to adsorbed-phase VOC-odor will occur for any airborne dust/VOC-odor composition. There are many complicating issues in developing this correlation, such as the difficulty in determining an appropriate partitioning coefficient and correlation to airflow velocity or adsorption rate coefficient.

It is likely that the heterogeneity of the physicochemical/biological characteristics of airborne dust/VOC-odor compositions and the resulting variability of adsorption rates was large, requiring the diversity of rate controls inherent in the sophisticated kinetic model for successful prediction of the adsorption and transport of VOC-odor in a ventilated airspace within a dusty medium.

Additional experiments are needed to establish the generality of the model. The implication of the present predictive model is that there are heterogeneous rate controls on the adsorption of the VOC-odor on the aerosol surface, and there are heterogeneous air mixing patterns that affect the residence time of airflow which consequently affect the effective performance of a ventilation system. Thus, this complex description of adsorption kinetics and incomplete mixing of air was required.

References

[1] R.H. Zhang, P.N. Dugba, D.S. Bundy, Laboratory study of surface aeration of anaerobic lagoons for odor control of swine manure, Trans. ASAE 40 (1) (1997) 185–190.
[2] J. Zhu, D.S. Bundy, X. Li, N. Rashid, Controlling odor and volatile substances in liquid hog manure by amendment, J. Environ. Qual. 26 (3) (1997) 740–743 1997.
[3] C.M. Liao, H.M. Liang, S. Singh, Exposure assessment model for odor causing VOCs volatilization from stored pig slurry, J. Environ. Sci. Health B 33 (4) (1998) 457–486.
[4] C.M. Liao, S. Singh, Modeling dust-borne odor dynamics in swine housing based on age and size distributions of airborne dust, Appl. Math. Modelling 22 (9) (1998) 671–685.
[5] C.M. Liao, J.S. Chen, J.W. Chen, Dynamic model for predicting dust-borne odour concentrations in ventilated animal housing, Appl. Math. Modelling 24 (2) (2000) 131–145.
[6] J. Zhu, A review of microbiology in swine manure odor control, Agric. Ecosyst. Environ. 78 (2000) 93–106.
[7] E.M. Barber, J.R. Ogilvie, Incomplete mixing in ventilated airspaces. Part I. Theoretical considerations, Can. Agric. Eng. 24 (1) (1982) 25–29.
[8] Y.C. Chen, E.M. Barber, Y. Zhang, R.W. Besant, S. Sokhansanj, Methods to measure dust production and deposition rates in buildings, J. Agric. Eng. Res. 72 (1992) 329–340.
[9] G.P. Box, G.M. Jenkins, Time Series Analysis: Forecasting and Control, Prentice-Hall, Englewood Cliffs, NJ, 1976.
[10] W.J. Weber, F.A. DiGiano, Process Dynamics in Environmental Systems, Wiley, New York, 1995.
[11] C.M. Liao, J.J.R. Feddes, A lumped-parameter model for predicting airborne dust concentration in a ventilated airspace, Trans. ASAE 35 (6) (1992) 1973–1978.
[12] O. Liu, S.J. Hoff, G.M. Maxwell, D.S. Bundy, Comparison of three κ–ε turbulence models for predicting ventilation air jets, Trans. ASAE 39 (2) (1996) 689–698.
[13] S.J. Hoff, D.S. Bundy, Comparison of contaminant dispersion modeling approaches for swine housing, Trans. ASAE 39 (3) (1996) 1151–1157.
[14] C.M. Liao, H.M. Liang, Characterization of mixing patterns in a ventilated airspace with a multiple airflow regions gamma model, J. Environ. Sci. Health A 36 (3) (2001) in press.
[15] J.W. Moore, R.G. Pearson, Kinetics and Mechanism, 3rd ed., Wiley, New York, 1981.
[16] Y.L. Yeh, C.M. Liao, J.S. Chen, J.W. Chen, Modeling lumped-parameter sorption kinetics and diffusion dynamics of odor causing VOCs to dust particles, Appl. Math. Modelling 25 (2001) in press.
[17] H. Stehfest, Numerical inversion of Laplace transforms, Commun. ACM 13 (1970) 47–49.
[18] A. Talbot, The accurate numerical inversion of Laplace transforms, J. Inst. Math. Appl. 23 (1979) 97–120.
[19] K.S. Crump, Numerical inversion of Laplace transforms using a Fourier series approximation, J. Assoc. Comput. Mech. 23 (1976) 89–96.
[20] F.R. de Hoog, J.H. Knight, A.N. Stocks, An improved method for numerical inversion of Laplace transforms, SIAM J. Sci. Stat. Comput. 3 (3) (1982) 357–366.
[21] IMSL MATH/LIBRARY, FORTRAN Subroutine for Mathematical Applications, vol. 1 and 2, Visual Numerics, Houston, Texas, 1994.